

Mass Modelling with Minimum Kinematic Information

Dalia Chakrabarty¹ *

¹ *School of Physics & Astronomy, University of Nottingham, Nottingham NG7 2RD, U.K.*

19 April 2018

ABSTRACT

Mass modelling of early-type systems is a thorny issue; even for the few close by galaxies for which kinematic data is available, the implementation of this data can get embroiled in problems that are hard to overcome, unless more complete data sets are available. The mass-anisotropy degeneracy is a typical example of this. In this paper, we present a new mass modelling formalism for ellipticals that invokes no other observations other than the central velocity dispersion (σ_0) and photometry. The essence of the method lies in choosing a local mass-to-light ratio (M/L) profile for a galaxy, with which the deprojected luminosity density distribution (along the major axis coordinate x) is scaled. The resulting discontinuous mass density profile is then smoothed, according to a laid out prescription; the local M/L profile that stems from this smoothed mass density, is found to be significantly different from the raw M/L distribution. A suite of model galaxies (both Sersic and cored in nature) is used for intensive experimentation in order to characterise this raw M/L profile and in each case, the mass density recovered from this mass modelling technique is compared to the known mass distribution. We opt to work with a raw M/L profile that is a simple two-stepped function of x , with a low inner and higher outer value of $M/L - \Upsilon_{in}$ and Υ_{out} , respectively. The only constraint that we have on this profile is in the centre of the galaxy, via σ_0 . This value of σ_0 is implemented in the virial theorem to obtain an estimate of the central M/L ratio of the galaxy. The fallibility of the virial mass estimate is taken care of, by allowing for a range in the values of Υ_{in} that can be used for a given galaxy model. Moreover, our experiments indicate that Υ_{out} is uniquely known, for a given Υ_{in} ; for cored galaxies, this functional form is found uniquely dependant on the core radius. The physical basis for such a connection to exist between the inner and out M/L is discussed. The jump radius of the raw M/L profile is chosen to be about thrice the effective radius of the galaxy. In this way, the local M/L distribution is completely specified and mass profiles of ellipticals can be constructed till about 3 times the effective radius. The proposed technique is extended to predict a mass profile for M87 which is then successfully compared to distributions reported earlier from kinematic analyses.

Key words: galaxies: kinematics and dynamics – galaxies: structure – celestial mechanics: stellar dynamics

1 INTRODUCTION

The recovery of the total mass distribution in early type systems is a knotty problem. The obvious reason for this is lack of information; photometry offers access to the stellar mass but the deduction of the arrangement of the total mass in a system remains elusive, unless kinematic information is invoked. Even when velocity information is available, the implementation of the same is besotted with problems of varying degrees of subtleness (Merritt 1993, Merritt 1996, Chakrabarty & Saha 2001, Genzel *et al.* 2000).

Of the many debacles that plague the processing of kinematics, the worst is perhaps the mass anisotropy degeneracy; even in the simplistic case of a spherical system, the mass distribution can be known only as a function of the anisotropy in velocity space (Binney & Tremaine 1987). Getting an independent handle on anisotropy is difficult, if not impossible in most cases. Côté *et al.* (2001) attempt this for the system of globular clusters in M87, by constraining the total mass from the work of McLaughlin (1999). Their conclusion indicates that the velocity distribution of this system in M87 is “almost perfectly isotropic”. This is consistent with the appraisal of isotropy in globular cluster systems in other galaxies (Zepf *et al.* 2000, Côté *et al.* 2003).

* E-mail:dalia.chakrabarty@nottingham.ac.uk

An attempt is also underway to produce a fully anisotropic algorithm, that is similar in flavour to the existing code CHASSIS that works by implementing kinematic data of tracers to recover the potential and distribution function from which the tracer sample is most likely to have been drawn (Chakrabarty & Saha 2001, Chakrabarty & Portegies Zwart 2004). However, a large number of kinematic observations is required by this proposed extension. Nonetheless, what is heartening is that such ambitious data sets are less of a figment of the astronomer’s reverie today, owing to the huge kinematic surveys that are planned or already in operation.

Another technique that is often employed in mass modelling of elliptical galaxies involves the utilisation of X-ray measurements. The procedure suffers from uncertainties in the observed temperature profile and simplification in terms of the assumption of a single component in the X-ray emitting gas and of hydrostatic equilibrium. A comprehensive review of various the shortcomings of the conventional mass modelling techniques is presented in Mamon & Lokas (2005).

Thus, it is clear that at the present moment, utilisation of kinematic information in mass modelling, suffers from egregious drawbacks. Even more crucially, such data is hard to come by in many external galaxies, including those at higher redshifts. For this latter class, the implementation of velocity information in formalisms that stem from a stellar distribution function, is all the more debatable since systems outside the local universe are most probably not relaxed.

This indicates an opening for a technique that is able to extricate the mass profile of early type systems from photometry, using as little velocity information as possible. Moreover, the used kinematic information should not be used in a procedure that relies on the rigorous employment of the equilibrium stellar distribution function. Such a scheme is advanced in this short report.

It merits mention that any such mass modelling formalism for elliptical galaxies will bear the potential of shedding light on the connection between the luminous and dark matter content in such systems. In the past, such correlations have been explored in spiral galaxies (Sancisi 2004, Verheijen 2001 and Noordermer 2006), but very little is known about the distribution of the total mass in ellipticals; Padmanabhan *et al.* (2004) and Lintott, Ferreras & Lahav (2006) discuss sample galaxies in this context. The scheme discussed here will indicate the same in model systems.

The paper is arranged as follows. The next section provides an exposure to the details of the proposed scheme. In Section 3, the Sersic model considered in the paper is introduced. Section 4 is devoted to the results obtained with the toy galaxy models, while the following section (Section 5) delineates the galaxy models that can be tackled with the proposed scheme from those that are outside the purview of this scheme. Section 6 discusses the details of the results obtained with the data for M87, as obtained from the ACS Virgo Cluster Survey (ACSVCS), (Ferrarese *et al.* 2006), and comparison of the recovered mass model with those predicted by Côté *et al.* (2001) and Romanowsky & Kochanek (2001), (from the analysis of kinematic data of tracer populations in M87). The last section is devoted to the discussions of some of the salient points that were raised in the other sections and a summary of the results.

2 DETAILS OF THE FORMALISM

We work under the assumption that the surface brightness profile of a galaxy is known to us. The central velocity dispersion (σ_0) is also considered known from observations.

2.1 Deprojection

The first step is to deproject the observed brightness profile into the three dimensional luminosity density distribution. This can be done with the non-parametric deprojection algorithm DOPING, which is the acronym for Deprojection of Observed Photometry using an INverse Gambit (Chakrabarty & Ferrarese 2006).

This algorithm can perform the deprojection under a general geometry that needs to be specified as an input. The other fundamental input is the inclination. The measurements that DOPING processes are the surface brightness measurements and the projected ellipticity profile, at different values of the major axis coordinate x , i.e. the surface brightness map of the galaxy. This is used to provide the three dimensional luminosity density distribution, the line-of-sight projections of which are the best reproductions of the brightness data, along any azimuth on the plane of the sky. The deprojection of the observed photometry for systems with varying intrinsic shape requires the implementation of a regularisation technique, though systems in which the ellipticity is uniform are more easily dealt with. It needs to be mentioned that DOPING can in principle, deal with changes of eccentricity and twist angle, with galactocentric distance.

The errors on the deprojected luminosity profile are the errors of the analysis, which measures the $\pm 1\text{-}\sigma$ extent of the excursion of the algorithm around the global maxima in the likelihood function; likelihood is maximised on spotting the luminosity density distribution that projects best into the data. The observational errors can be also incorporated into the analysis.

2.2 Models

In this paper, we attempt to mass model a set of toy elliptical galaxies. In terms of measurable quantities, these model systems are ascribed a brightness profile $I(x)$ and a projected ellipticity ϵ , that we choose to fix at 0.4, (implying that for edge-on viewing, the intrinsic eccentricity $e=0.8$). All the toy galaxies are assumed to have been observed in the SDSS I -band and placed at the distance of Virgo (considered as 17Mpc).

Multiple runs are carried out with the toy galaxies being assigned varying values of central velocity dispersion (σ_0), from which the local mass-to-light ratio at the centre of the galaxy is calculated in a way discussed below. These observables are the inputs into the mass modelling system that is proposed in the paper. The recovered total mass density distribution is then compared to the true mass density profiles ($\rho_t(x)$) of these models. The degree of overlap between the predicted and known mass distributions is then visually tracked, in order to confirm the success and limitations of the proposed mass modelling scheme.

The models are described by a luminous component (luminosity density $L(x)$) lying embedded in a dark halo that is

chosen to be NFW type (density: $\rho_{NFW}(x)$). Thus, the true total mass density of a model galaxy can be written as:

$$\rho_t(x) = \rho_{NFW}(x) + \alpha 10^{\frac{L_\odot - L(x)}{2.5}}, \quad (1)$$

where the dark matter density is

$$\rho_{NFW}(x) = \frac{M_s}{4\pi x(x + r_s)^2} \quad (2)$$

and α is a measure of the luminous matter fraction, such that its reciprocal indicates the halo fraction in the toy galaxy. Also, L_\odot is the absolute magnitude of the Sun in the same waveband as the brightness observations.

We treat two sets of model brightness distributions: the cored and the Sersic type profiles. As far as the cored brightness distributions are concerned, the following prescription is used. The brightness profile of the test galaxies is extracted from the line-of-sight integration of an analytically chosen luminosity density function. (Thus, the deprojection of this brightness data can be compared to the known luminosity density to confirm the correctness of the deprojection). This analytical luminosity density distribution $L_t(x)$ is chosen to have the form:

$$L_t(x) = \frac{A}{[r_c^2 + x^2 + y^2/(1 - e^2) + z^2]^{1.5}}, \quad (3)$$

where A is the central luminosity density and r_c the core radius of the test galaxy in question. Thus, various toy surface brightness data sets are prepared, with varying amplitude and core radii. The deprojection is carried out under the assumptions of oblateness and an edge-on viewing angle.

We normalise the deprojected luminosity density profiles of all the model galaxies such that the central value of $L(x)$ is about $100 L_\odot \text{pc}^{-3}$, leaving the models distinguishable from each other in terms of the core radius only. Each such model luminosity density profile is then ported to the mass modelling formalism (discussed below) and the outcome is compared to the known mass density distribution of this toy galaxy. Figure 1 shows the normalised luminosity distributions of the cored galaxies (of core radius 7.07pc and about 22.4pc) that have been used in our experiments.

For the Sersic models, the brightness is chosen to be described by a Sersic index of 5.3 and a scale length of about 108pc. This central density is normalised to $1000 L_\odot \text{pc}^{-3}$, i.e. 1 order of magnitude higher than the normalisation factor for the cored galaxies.

2.3 Raw Two-stepped Discontinuous M/L Profile

Once the deprojection is performed, the next stage is to choose a total *local* mass-to-light ratio (M/L) profile that scales the obtained luminosity density profile in such a way that it would hopefully emulate the total mass density. Or at least, such is the aim, as in other procedures that hope to connect photometry to a mass model. We suggest selection of a discontinuous, two-step local M/L :

$$\begin{aligned} M/L &= \Upsilon_{in} & \text{if } x \leq x_{in} \\ M/L &= \Upsilon_{out} & \text{if } x > x_{in} \end{aligned} \quad (4)$$

The luminosity density is scaled by this mass-to-light ratio profile and then *smoothed*. Of course, the success of the scheme depends on the selection of x_{in} , Υ_{in} and Υ_{out} .

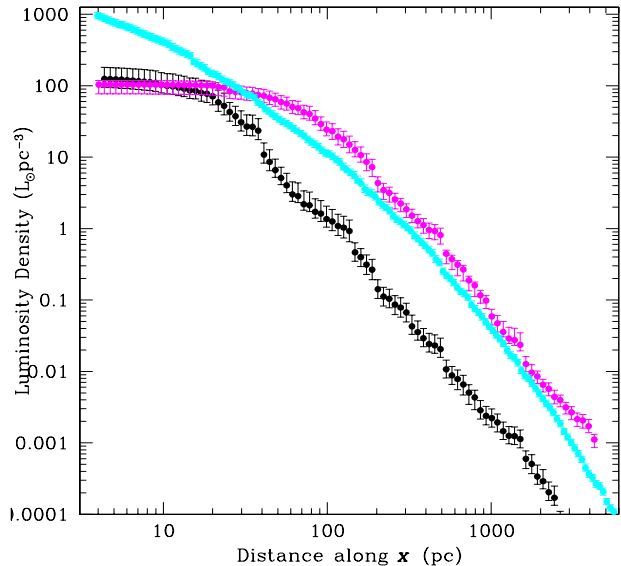


Figure 1. Deprojected luminosity density profiles of toy galaxies with core radii of about 7.1pc (in black) and 22.4pc (in magenta), recovered by DOPING from model brightness profiles that were constructed from the analytical luminosity distribution given in Equation 3, normalised to $100 L_\odot \text{pc}^{-3}$. The Sersic luminosity density is shown in cyan, normalised to $1000 L_\odot \text{pc}^{-3}$.

Additionally, we need to be cautious that this method is susceptible to spurious answers at distances where the dark matter halo dominates the system. Thus, we aim to produce a mass profile over a radial range that is not too extensive (not exceed about $3X_e$, where X_e is a measure of the effective radius of the galaxy). We ascertain X_e by measuring the slope (m) of the straight line that is fit to the plot of core-removed $\log_{10}(I)$ against $x^{1/4}$: $X_e = (-3.33/m)^4$.

So, what would amount to a judicious prescription for the selection of the free parameters in this formalism? If we were to assume that mass follows light in elliptical galaxies, then we could set $\Upsilon_{in} = \Upsilon_{out}$ and x_{in} could be set to any value in the range of $[0, 3X_e]$. But there is no reason to believe that mass does follow light in elliptical galaxies. In fact, gas kinematics and X-ray studies indicate otherwise; Buote *et al.* (2002) report that the hypothesis that mass follows light can be rejected at 96% for their oblate models for NGC720 and 98% for their prolate models. Bertola *et al.* (1993) point out that the run of the mass-to-light ratio with galactocentric radius in ellipticals is similar to that in spirals.

Kinematics too rule out the possibility of a constant M/L at 95% confidence (Gerhard *et al.* 2001). More recently, the analysis of the kinematics of planetary nebulae observed in five elliptical galaxies, by the Planetary Nebula Spectrograph, has led to the announcement that these galaxies are drastically short of dark matter in the outer parts (Romanowsky *et al.* 2003, Romanowsky *et al.* 2004). Napolitano *et al.* (2005) advance a parameter that measures the logarithmic slope of the mass-to-light ratio in a sample of early type galaxies, to find that it increases with the stellar mass. They conclude that the distribution of dark matter or its fraction changes with radius.

2.3.1 Jump Radius

Thus, we are left to make as good a choice for the parameters as possible, from whatever can be learnt about the system from the minimum of observables. Now, there is no observational constraint that can suggest a value for the jump radius x_{in} , at which the above two-step local M/L profile should suffer its discontinuity. However, one obvious length scale in the problem is X_e . So we can choose to impose a certain multiple of X_e as the jump radius; in fact, experiments indicate that a good value of x_{in} is $3X_e$. This is not a particularly bad choice either, given that by 3 effective radii, the dark matter content can be expected to begin to exert its influence. Having fixed x_{in} , we now proceed to use whatever observable information there may be available to constrain Υ_{in} and Υ_{out} .

2.3.2 Inner M/L

One measure that is often available from observations is the central velocity dispersion in galaxies. σ_0 can be utilised to get a handle on the local mass-to-light ratio in the inner parts of the galaxy (i.e, Υ_{in}). This can be done by implementing σ_0 that is measured at $x = x_0$ (say), in the virial theorem. However, the estimation of the mass enclosed within x_0 (M_0), from which the average mass density (ρ_0) inside x_0 can be calculated in this way, will be mired in errors owing to a lack of information about the degree of anisotropy present at $x = x_0$, as well as the extent of deviation from sphericity at x_0 . Virial theorem suggests that under the assumption of velocity isotropy,

$$3\sigma_0^2 = \frac{GM_0}{\frac{1}{2}x_0} \quad (5)$$

and oblateness and edge-on inclination imply

$$M_0 = \frac{4\pi}{3}\rho_0 x_0^3 \sqrt{1 - e^2} \quad (6)$$

This estimated ρ_0 will deviate from the true inner mass density, as explained above. Anisotropy will spuriously lower the estimated enclosed mass and therefore the calculated ρ_0 , for a given σ_0 . For example, Padmanabhan *et al.* (2004) suggest that the dynamical mass enclosed within the projected half-light radius (R_e) of the massive ellipticals in their SDSS sample is given as 1.65² times $\sigma_0^2 R_e/G$, with a systematic error of 30% (Lintott, Ferreras & Lahav 2006).

Expectedly, the central M/L ($M/L(0)$) has a one-to-one and monotonically increasing relationship with the luminous matter fraction index α (lower left panel of Figure 2). As shown in the figure, $M/L(0)$ is well represented by α , though the deviation of $[M/L(0)]/\alpha$ from unity exists - this ratio decreases from about 0.22 to 0.07 as we increase r_c from 7.1pc to 22.4pc. *We will use this result to justify our choice of α for parametrising the estimated central M/L .*

We scan through a range of estimated central M/L values (i.e. α) and monitor the success of the proposed technique; in the process, the ranges of Υ_{in} and Υ_{out} corresponding to a given choice of the central M/L value are recorded.

Now, experiments with our model galaxies of a given core radius r_c indicate that for a given α , there exists a range of values for Υ_{in} that will result in compatibility of the estimated and known mass density profiles (upper left panel in Figure 2). This band of allowed Υ_{in} values for a given α ,

varies with core radius of the normalised luminosity density profile in hand. For our cored galaxies, this band of Υ_{in} values that are allowed at a given α , range from just above the corresponding value of α to approximately 2 times this α , with this factor varying only weakly with core radius r_c .

If we assume the value of 2.72 between the true value of the mass enclosed within an effective radius and $\sigma_0^2 R_e/G$, as suggested by Padmanabhan *et al.* (2004) (and used by Lintott, Ferreras & Lahav 2006), then the true central M/L should be about 1.82 times the virial estimate. Thus, the range of 2α that is allowed in Υ_{in} , for a given estimate of $M/L(0)$, appears to be inclusive of real ellipticals, at least the systems that are as massive as those in the sample of Padmanabhan *et al.* (2004).

If it so happens that a certain galaxy is far too anisotropic at the centre, such that the true $M/L(0)$ exceeds the upper bound on the Υ_{in} allowed at the α at hand, then the mass density profile that will result from using the highest value of the permitted Υ_{in} in our mass modelling formalism, will not concur with the profile that results from using the lowest allowed Υ_{in} . Thus, in such circumstances, when our scheme fails, we will be aware that it has done so.

Thus, it may be summarised that even though the virial theorem is invoked to help constrain Υ_{in} , there is enough scope available within the formalism to accommodate for the problems caused by velocity anisotropy in traditional kinematic modelling. This and other flexibilities offered by the proposed formalism are discussed in greater detail in Section 7.

2.3.3 Outer M/L

Our experiments indicate that it is possible to achieve a one-to-one correlation between Υ_{in} and Υ_{out} , for a toy configuration of a given core radius. In other words, irrespective of α , whenever a value of Υ_{in} is chosen, Υ_{out} is fixed. This relationship between Υ_{in} and Υ_{out} is depicted on the top right panel in Figure 2.

Actually, there exists a range of Υ_{out} for a given Υ_{in} , with the extent of this range maximising itself at values of Υ_{in} that lie in the middle of the range that is allowed for a given α . However, to keep matters simple, we present only the value of Υ_{out} that lies at an extrema of this range, for a given Υ_{in} .

Analytical fits to the plots suggest that Υ_{out} varies as $A_1 \exp[-\Upsilon_{in}/\tau] + A_0$, where A_1 and A_0 are constants that are determined from fitting this exponentially decaying function to the plot of Υ_{out} against Υ_{in} ; τ measures the decay rate. Fitting this functional form to the experimentally obtained plots, suggest power-law dependences of both the additive and multiplicative constants, on r_c :

- (i) $A_1 \sim r_c^{-5.31}$,
- (ii) $A_0 \sim r_c^{-3.75}$ and
- (iii) τ has a weak dependence on r_c , according to $\tau = 1.005^{-6} r_c^4 + 1.85$.

That the inner and outer local M/L ratios are connected, betrays a relationship between the luminous and dark matter content in these toy elliptical galaxies. This facet of the models and the conclusions that we can draw on the basis of these results for elliptical galaxies in general, are further explored in Section 7.

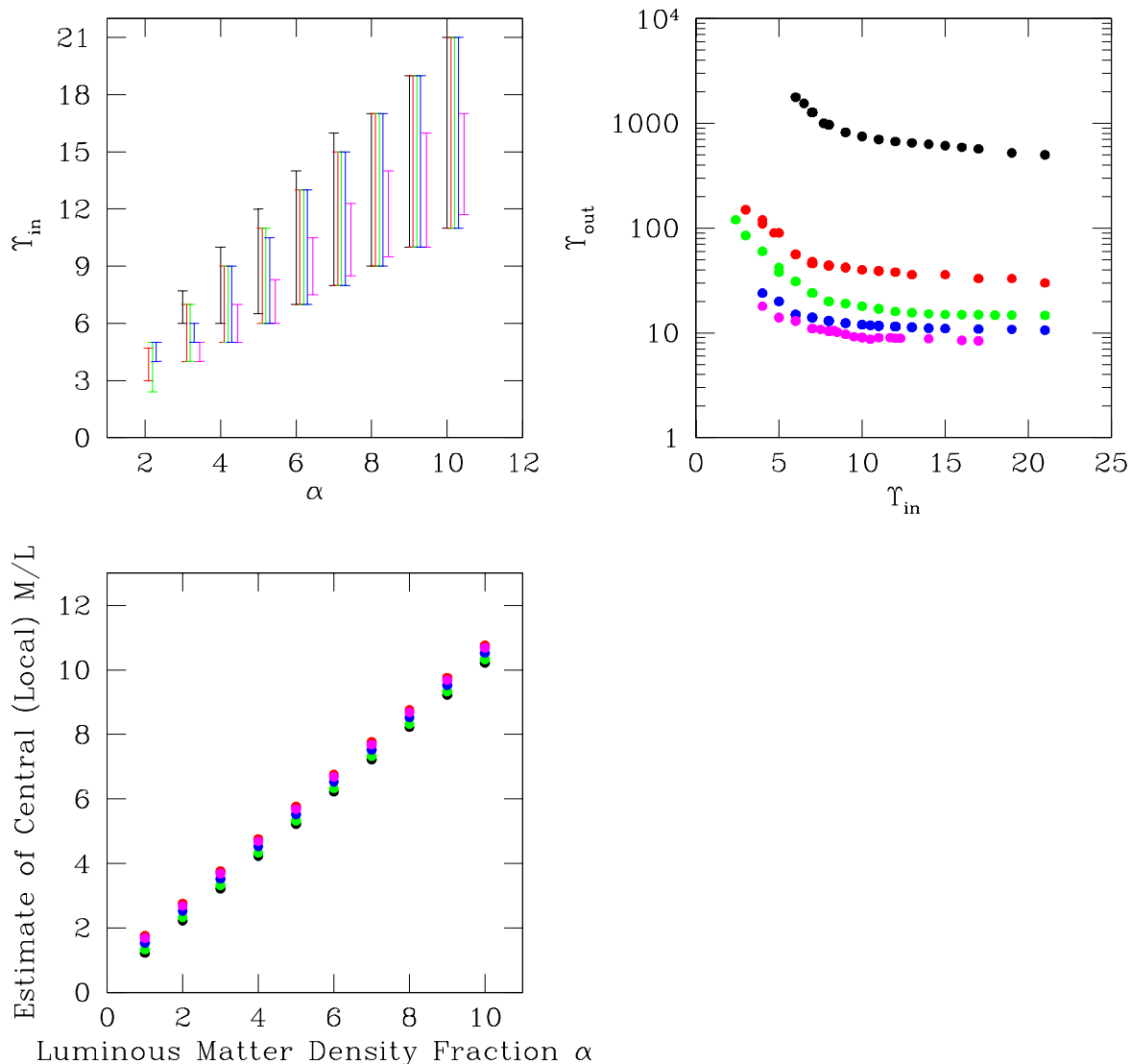


Figure 2. Lower left panel: the luminosity matter fraction α , plotted as a function of the estimated central M/L . Results for $r_c=7.1$ pc are shown in black, for 14.4pc in red, for 17.3pc in green, for 20pc in blue and for 22.4pc in magenta. Top left panel: figure showing the allowed ranges in Υ_{in} , as a function of α (which measures the estimated central local M/L), for cored galaxies of varying core radii; the colour indexing used here is the same as above. Top right panel: Υ_{out} plotted as a function of Υ_{in} .

2.3.4 Smoothing

Once the local M/L is specified, it is used to scale the luminosity density distribution, in order to obtain a mass density distribution, which is indeed rendered discontinuous by the process of its formulation. Thus, the next stage is to smooth this mass density distribution.

We choose to smooth this density profile with a triangle filter of filter size given by $2X_e$, i.e. two successive applications of a box filter of filter size corresponding to the length X_e . It is appropriate that the smoothing filter size be a function of one of the characteristic scale-lengths of the system; X_e is the most obvious candidate that satisfies this criterion. Thus, the trends in Υ_{out} with variation in Υ_{in} , for the different normalised toy galaxy configurations, have

been extracted from experiments performed with a smoothing filter size of X_e . However, other smoothing windows are also usable - except that the exact nature of the relationship between Υ_{out} and Υ_{out} will then be different from what is prescribed above, for a given r_c .

3 SERSIC GALAXIES

All the toy models that are discussed above correspond to examples of surface brightness profiles that are cored. In order to investigate the full applicability of our mass modelling technique, a Sersic type galaxy is now examined.

We consider a toy Sersic surface brightness distribu-

tion, described by a central density of $1000 L_{\odot}\text{pc}^{-3}$, a scale length of about 100pc and a Sersic index of 5.3 . When deprojected under the assumption of sphericity, a luminosity density profile along the semi-major axis is recovered. The central density chosen for this toy model is $1000 L_{\odot}\text{pc}^{-3}$ instead of $100 L_{\odot}\text{pc}^{-3}$ (as in the cored models), since the proposed mass modelling technique does not work for Sersic models at the lower normalisation.

Once normalised in this way, a range of central (local) mass-to-light ratio values are imposed, in order to scan the range of parameters over which our scheme is viable. As before, the central M/L values are imposed in terms of the parameter α (the luminous matter fraction). The raw two-step local M/L profile that is imposed upon this luminosity density is again chosen to be described by an inner M/L of Υ_{in} and an outer M/L of Υ_{out} , with the jump radius given by $3X_e$.

In these Sersic models, X_e is defined as the slope (m) of the straight line that is fit to the plot of $\log_{10}(I)$ against $x^{1/4}$: $X_e = (-3.33/m)^4$. For the toy model at hand, we find $X_e \approx 726.8\text{pc}$.

Once the two-stepped local M/L profile is fully characterised, the deprojected luminosity density is scaled by it and the resulting mass density distribution is smoothed. As before, it is smoothed by two successive applications of a boxcar smoothing filter of filter size given by X_e .

For a given choice of the central M/L , a range of Υ_{in} are allowed. This is shown on the left panel of Figure 3. This range is evidently smaller for the Sersic toy model, compared to the cored models. Again, we find that a one-to-one relationship exists between Υ_{in} and Υ_{out} , as shown in the right panel of Figure 3.

Thus, it is apparent that galaxies with brightness distributions that are best described by a Sersic profile, can also be tackled by the proposed mass modelling scheme. The two main differences in the formalism, as applicable to the cored and Sersic brightness profiles are the following.

- (i) The luminosity density for a Sersic-type galaxy needs to be normalised to $1000 L_{\odot}\text{pc}^{-3}$, while a cored brightness profile would require a normalisation factor that is 1 order of magnitude smaller.
- (ii) For the determination of X_e of the Sersic-type galaxies, a straight line fit to the plot of $\log_{10}(I)$ against $x^{1/4}$ needs to be performed while for the cored galaxies, a linear fit is sought to the relationship between the *core-removed* $\log_{10}(I)$ profile and $x^{1/4}$.

4 RESULTS

Figure 4 brings out the change in the local mass-to-light ratio profile, as a result of the smoothing; the mass density distribution that results from the smoothing of the scaled luminosity density profile, is compared to the luminosity density, to extract the smoothed local M/L . This is seen in the figure to be different from the raw, two-step, discontinuous M/L distribution that is used to scale $L(x)$. The smoothing is noted to affect mass-to-light on both sides of the jump radius.

Figure 5 displays the degree of overlap between the estimated and true mass density profiles, for toy cored galaxies that are normalised to the same central luminosity density

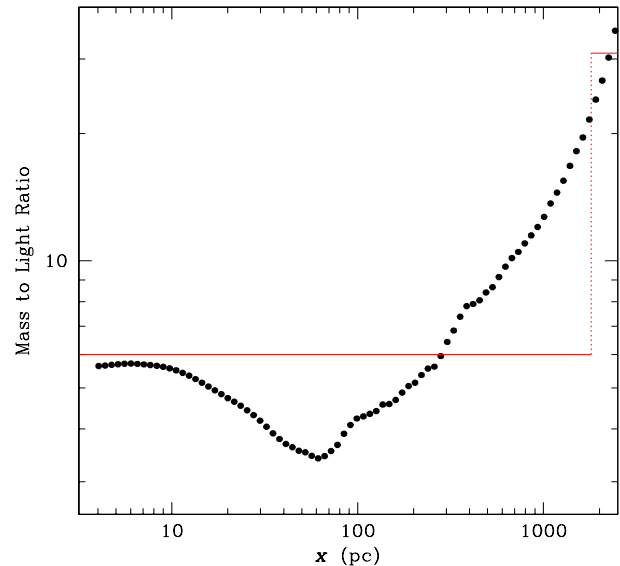


Figure 4. Plot of the raw (in broken red lines) two-stepped local M/L ratio that is used to scale the luminosity density profile of the toy galaxy of core radius 17.3pc , given model parameters of $\alpha=3$, $\Upsilon_{in}=6$ and $\Upsilon_{out}=31$. The resulting discontinuous mass density profile is then smoothed according smoothing prescription mentioned above. When this smoothed mass density distribution is compared to the deprojected luminosity density profile, the resulting local M/L profile is shown in filled circles. As is apparent, the raw two-stepped M/L distribution varies significantly (beyond error bars) from the final smoothed M/L ratio distribution.

and characterised by varying shapes, i.e. varying r_c (upper panels). The lower panels of the same figure indicate a similar comparison, when α is made to change. In all these cases, when we utilise the prescribed values of Υ_{in} and Υ_{out} , the predicted mass density profile reproduces the true mass density profile very well, within error bars.

Figure 6 brings out the resemblance between the known mass density distribution along the major axis (in green) and its predicted counterpart (in red), for the Sersic model investigated, for a value of Υ_{in} that is picked from the range allowed for a given choice of the estimated central M/L .

5 ALLOWED GALAXIES

This scheme of characterising the two-step local mass-to-light ratio profile is found to work only as long as the galaxies at hand lie within a certain band in the $M_s - r_s$ space, where M_s is the mass scale and r_s is the scale radius that describe the NFW dark halo mass density profile (see Equation 2). This band is translated into a range of the allowed values for the cored galaxies, in the $V_{200} - r_s$ space, (where V_{200} is the circular velocity at radius r_{200}), in Figure 7. The broken line in this figure indicates the state of the NFW halos, as given in Hoekstra, Yee & Gladders (2004). The range in M_s allowed for Sersic-type galaxies is slightly more constricted, as compared to the cored galaxies.

To clarify, by these “allowed ranges”, we imply the ranges in V_{200} and r_s , over which the same Υ_{in} and Υ_{out} values are valid.

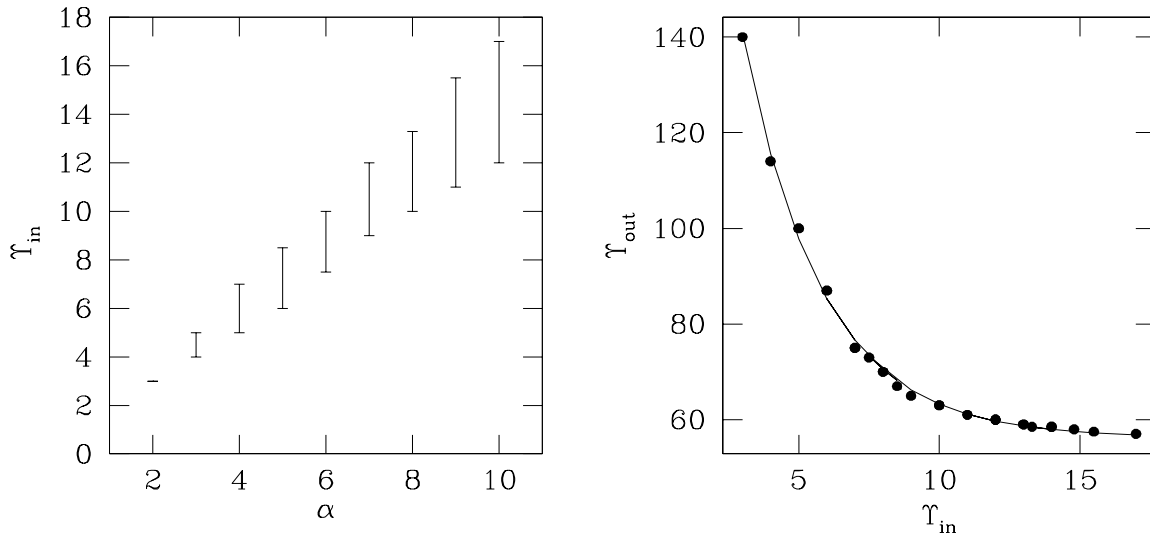


Figure 3. Left panel: the allowed ranges in Υ_{in} , as a function of the estimated central local M/L , as parametrised by α , for the Sersic model that we consider. Top right panel: Υ_{out} plotted as a function of Υ_{in} ; the solid line represents an exponentially decaying function of Υ_{in} that is a very good fit to our experimentally obtained data.

Thus, it is apparent that the mass modelling scheme that is being proposed here is applicable even to systems that may exhibit a significant range in concentration. At the same time, we note that dwarf galaxies which typically have $V_{200} \sim 100 \text{ kms}^{-1}$ cannot be characterised by this formalism.

In addition to these constraints on the M_s and r_s , the galaxies also need to be “ordinary” in the sense that they should, qualitatively speaking, have a lower inner mass-to-light ratio than a higher M/L at higher radii. However, if the galaxy at hand is known to have a central mass condensation from independent measurements (such as M87), the raw two-step M/L profiles discussed above (described by a low Υ_{in} and a Υ_{out}) will not be apt. We refer to such galaxies as “not ordinary” in this paper. For such a system, an alternative three-step, local mass-to-light profile can be conjured. In such a configuration, the value of the M/L in the innermost region must be retained as high, while the intermediate range is envisaged to be described by a low M/L . Outside of the second jump radius, the dark matter contribution is expected to kick in; therefore, the mass-to-light ratio in the outermost part should be held at a high value. The values of the M/L in the different parts of such systems are not expected to be given according to the prescriptions mentioned above; nor are the two relevant jump radii in these cases, expected to be given as multiples of X_e in the same way as for “ordinary” galaxies.

In general, the mass modelling of such systems are beyond the scope of the proposed formalism. Nevertheless, in Section 6, we will show how the basic concept behind our proposed mass modelling formalism can be extended to model M87, using whatever we know of the physics of M87, from literature.

6 M87

In this section, we present a mass model of the galaxy M87. We compare our results with the enclosed mass profile put forward by Côté *et al.* (2001) and the mass density of M87, suggested by Romanowsky & Kochanek (2001).

M87 (NGC 4486) is a cD galaxy that lies near the centre of the Virgo cluster. It has been extensively studied both for the photometry of its stars and its globular cluster system (Strom *et al.* 1981) as well as for their kinematics; some of the latest investigations are due to Romanowsky & Kochanek (2001), Côté *et al.* (2001). M87 is marked by the existence of a central supermassive black hole (Macchetto *et al.* 1997, van der Marel 1994) and a dearth of dark matter in the outer parts; we configure the details of the raw M/L profile accordingly.

Given that M87 is “not ordinary”, according to the prescription suggested in the previous section, it is expected to require a three step discontinuous raw M/L profile, in which the local M/L in the innermost step is high (in conjunction with the reported central supermassive black hole) and that in the intermediate and outermost steps are expected to be moderate and high respectively. However, given that M87 has been modelled with no dark matter halo in the past (McLaughlin 1999), with most of its dark matter being that of Virgo, it makes sense for us to maintain the same value of the local M/L in the outer two steps (at least upto the radius to which photometric information is available). Thus, the raw M/L profile is rendered two stepped and we are required to judiciously choose the jump radius x_{in} that marks the end of the regime where the influence of the central black hole dominates. The details of the choice of this raw M/L profile are discussed below:

- x_{in} is chosen to be $0.2''$; the ACS surface brightness profile of M87 indicates a steepening of the profile from about $0.2''$ inwards.

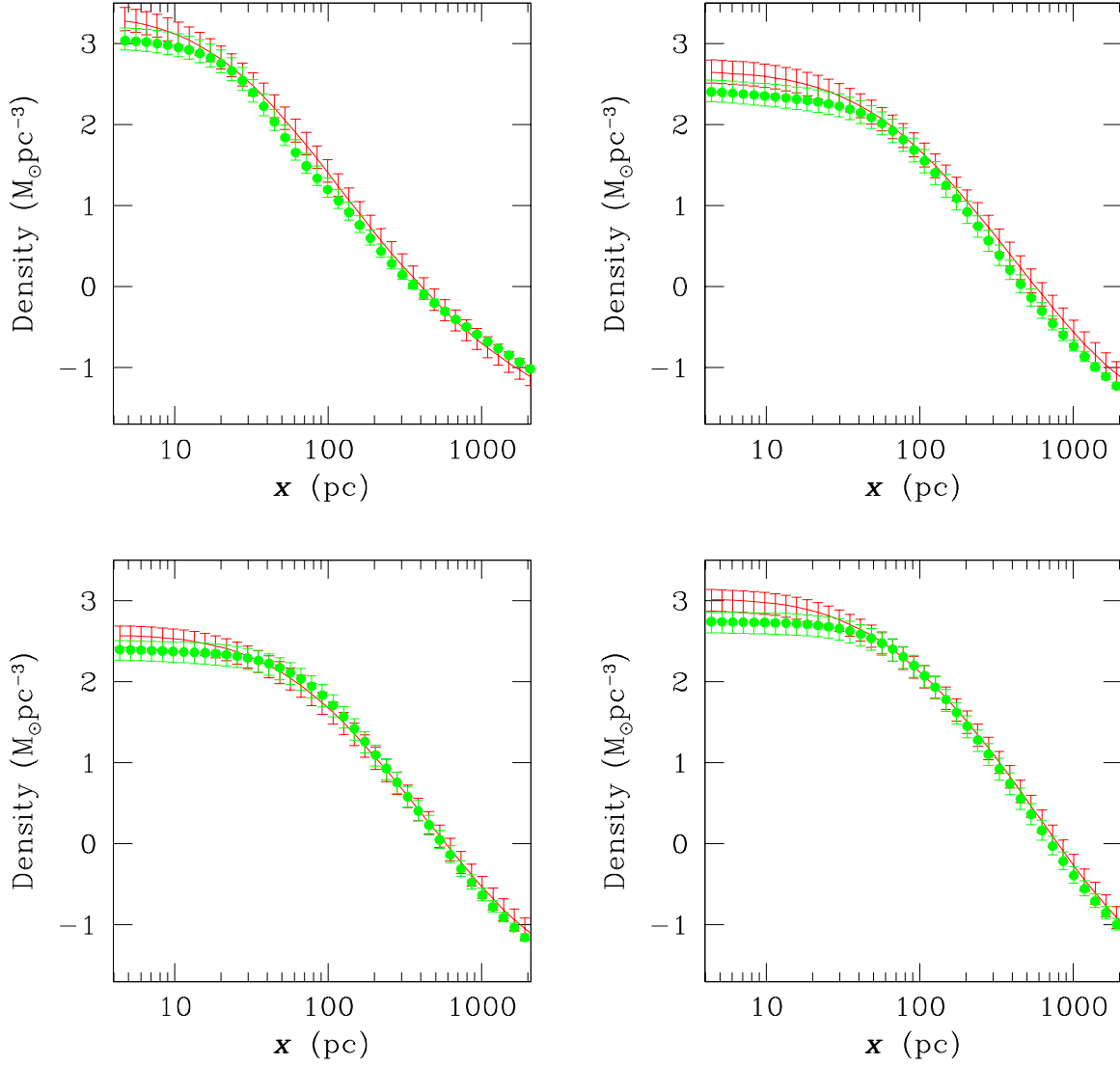


Figure 5. Comparison of recovered (in red) and model (in green) mass density profiles for the cored toy galaxies with varying α (lower panels) and core radii (upper panels). The two different core radii corresponding to the plots on the upper right and left are about 17.3pc and 7pc, respectively. These toy configurations have been ascribed the same α of 10. The lower right and left panels correspond to the same r_c of 20pc and $\alpha=3$ and 7, respectively. The range of x over which the profiles are shown corresponds to thrice the X_e for the $r_c=20$ pc model. This is in excess of $3X_e$ for the models with the lower core radii. That the overlap between the recovered and true profiles is notable over this whole x range, even in the cases of $r_c=17.3$ pc and 7pc, reflects the realisation that the mass modelling is often successful even beyond $x = 3X_e$.

- Outside the central $0.2''$, the mass to light ratio is considered to be constant, with a moderately large value of about 10. This is maintained till the end of the radial range to which the photometric data extends (about $100''$), which is just slightly higher than the X_e of about $96''$. We find that the allowed range of this intermediate M/L is 6 to 13.

- The observed central line-of-sight velocity dispersion of M87 (van der Marel 1994) is about 400kms^{-1} . This translates to an enclosed mass of about $1.6 \times 10^9 M_\odot$. Comparison with photometry implies a local central M/L of about 200.

Now, let us discuss the predicted mass models for M87,

against which the recovered profile is checked. Romanowsky & Kochanek (2001) adopt an orbit modelling approach to infer the mass density, from measurements of velocities of stars (to about 1.5 effective radii) and globular clusters (to about 5 effective radii). The available surface brightness and kinematic observations of the stars and globular clusters over assorted radial ranges were used in this work. Romanowsky & Kochanek (2001) use the Schwarzschild orbit library method to work with generalised mass models that include a contribution from the luminous matter; this is represented by the luminosity density $\nu_*(r)$ that is scaled by the M/L . The

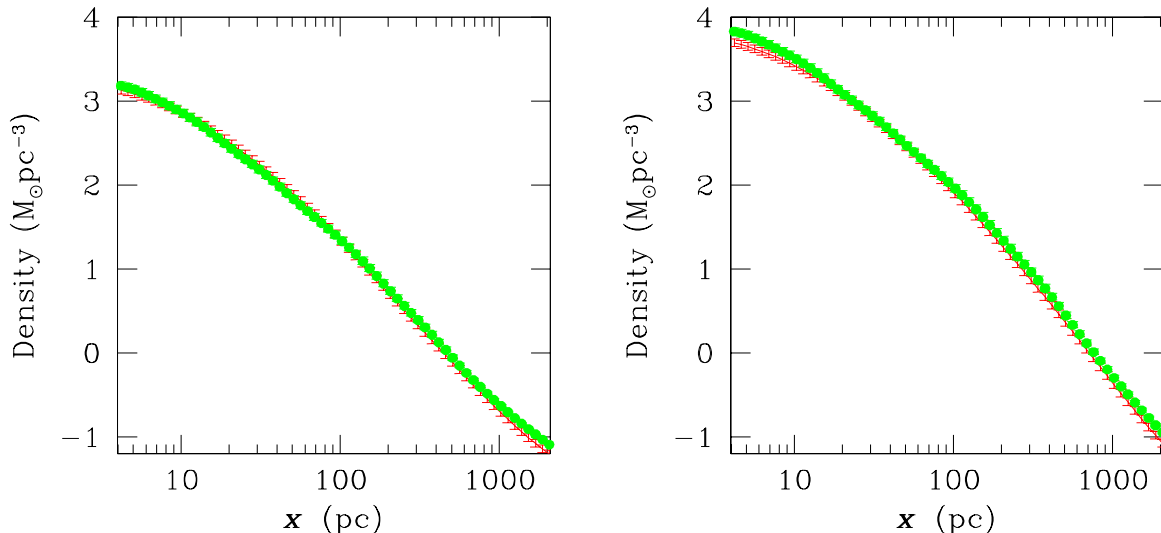


Figure 6. Similar to Figure 5, except that in this case, the comparison is shown for two distinct Sersic models that have been ascribed α of 2 (left) and 9 (right).

dark matter density is considered to be NFW type. The fitting is conducted on the joint constraints from the stellar and globular cluster velocity data, in a Jeans equation formalism. In this work, the availability of only one component of the velocity vector (the line-of-sight component), must render a wide range of solutions possible.

The best fit model from Romanowsky & Kochanek (2001) is presented in the right panel in Figure 8 in green. Even this best fit model is reported to suffer from the ailment that the values of the normalisation of the M87/Virgo mass profiles, as obtained from the stellar and globular data sets separately, are unequal. This could be explained by either a larger, less concentrated halo or by the relaxation of the assumption of sphericity. In fact, the ACSVCS image of M87 shows clearly that the eccentricity in M87 is not zero; the eccentricity is seen to dip sharply in the inner regions and then appears to tend towards a maximum of about 0.4, as radius increases.

The dynamical analysis of the radial velocities of 278 globular clusters of M87 is presented in Côté *et al.* (2001). The total (projected) radial range spanned by the kinematic data set of Côté *et al.* (2001) extends from about $36''$ to about 6.5 effective radii. This kinematic data is then fed into the Jeans equation under the assumption of a *spherical geometry*. In order to evade the problem of mass-anisotropy degeneracy, Côté *et al.* (2001) take the distribution of the total mass of M87 and the Virgo cluster that was deduced by McLaughlin (1999). This enclosed mass distribution is shown in black in the left panel of Figure 8. In this model, the dark matter is assigned wholly to the cluster.

The surface brightness and eccentricity profile of M87, observed as part of the ACS Virgo Cluster Survey were used as inputs to DOPING which recovered a luminosity profile for the galaxy. When the inferred light distribution is scaled by the two step M/L profile discussed above, and the consequent discontinuous mass density distribution is smoothed

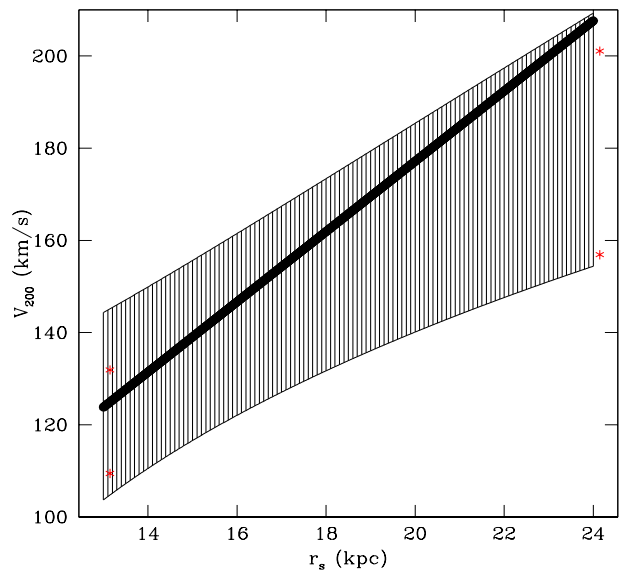


Figure 7. The shaded region indicates the section of the $V_{200}-r_s$ plane that corresponds to galaxy configurations that can be successfully modelled with the proposed mass modelling scheme. The solid black line is the NFW prediction, according to Hoekstra, Yee & Gladders, (2004). The red stars mark the extremes of the ranges in V_{200} and r_s that are allowed for the Sersic model considered in the paper.

(according to the smoothing prescription suggested in Section 2.3.4; smoothing filter size corresponds to x_{in}). The smoothed mass density profile is used to extract the enclosed mass profile, which is compared to the enclosed mass distribution of M87 that has been predicted by Côté *et al.* (2001) (see Figure 8). The comparison appears favourable indeed though the comparison of the recovered mass den-

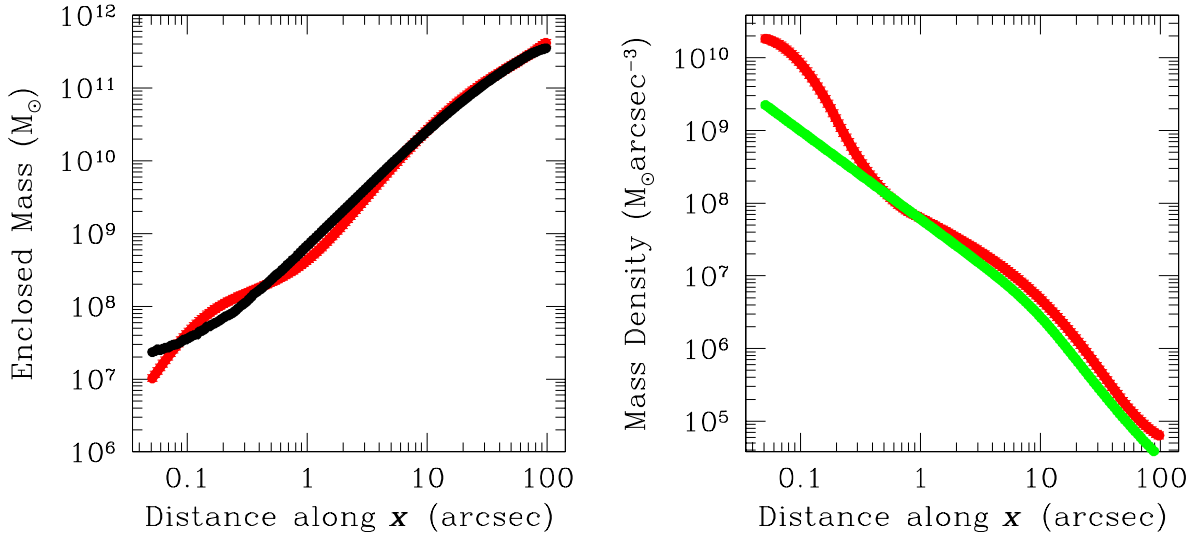


Figure 8. Figure showing the enclosed mass profile (left), and mass density (right) of M87. The ACS photometry for M87 is deprojected by DOPING to result in the luminosity density distribution of this galaxy. The recovered luminosity density is then scaled by a raw two-step local M/L profile that has a jump radius of $0.2''$, $\Upsilon_{in}=200$ and $\Upsilon_{out}=6$. The resulting discontinuous mass density distribution is smoothed (two successive applications of a boxcar smoothing filter of filter size 26 which corresponds to the jump radius of $0.2''$). This smoothed mass density distribution (in red) is compared (in the right panel) to that predicted by Romanowsky & Kochanek (2001) (in green). The enclosed mass profile that is calculated from this recovered mass density profile is shown in red in the left and is compared to the predictions of Cote et. al (2001) (in black).

sity to that predicted by Romanowsky & Kochanek (2001) is less encouraging in the central parts of the galaxy. This discrepancy however does not reflect badly on our mass modelling technique since the density predicted by Romanowsky & Kochanek (2001) is also in deficit of the enclosed mass predictions of Côté *et al.* (2001), due to the lack of inclusion of a central black hole in their model.

7 SUMMARY AND CONCLUSIONS

We propose a scheme to retrieve the total mass density to about 3 times the effective radius in ellipticals, using nothing but photometry and the central velocity dispersion: the exact two measurements that are most commonly available for most galaxies. The basic framework of this formalism relies upon the construction of a two-step, discontinuous, local M/L profile, which is chosen to suffer its discontinuity at $3X_e$. Here, X_e is the major-axis coordinate equivalent of the effective radius, as defined in terms of the fitting of the observed brightness profile to the de’Vaucouleurs $R^{1/4}$ law. Prescriptions are offered for constraining the inner and outer amplitudes of this sought two-step M/L profile. While Υ_{in} is found to lie within an allowed range of mass-to-light values for a given estimate of the central mass-to-light in the system, Υ_{out} is fixed for a given Υ_{in} , for a galaxy of a given shape. The details of the prescriptions are found to differ slightly, depending on whether the observed surface brightness is noted to be cored or Sersic in nature.

This formalism is designed to accommodate for the usual problems that are associated with our lack of knowledge of the state of anisotropy in the system and deviations

from sphericity. Thus, the measured central velocity dispersion is implemented in the virial theorem to pin down the (local) central mass-to-light ratio, but the possibility of miscalculating the same due to anisotropy always exists. However, this mistake can be covered for, to some extent, in the sense that as long as the true central mass-to-light ratio (Υ_{in}) lies within a range above the estimated central M/L (parametrised by α), the recovered mass density profile is found to be compatible with the true distribution. This range is given as 2α , the central luminosity density of which is normalised to $100 L_{\odot}pc^{-3}$. If on the other hand, the brightness profile is Sersic type, the normalisation factor is $1000 L_{\odot}pc^{-3}$ and for the only Sersic model that was explored, the upper bound on the allowed range for Υ_{in} is relatively more constricted, viz. 1.65 times α . A one-to-one relationship between Υ_{in} and Υ_{out} exists in both cases.

Such a prescription can fail if the degree of anisotropy in the centre of the system is so high that the virial estimate of the central mass density is rendered different from the true central density by a factor in excess of 2α in the case of cored galaxies and 1.65α , for Sersic galaxies. The good news is that when this happens, the formalism can indicate the same; such configurations cannot be handled by the proposed scheme. However, it is unlikely that the galaxy will be this anisotropic at the centre since a careful analysis of a sample of over 2000 galaxies in SDSS indicates that the dynamical mass enclosed with $1R_e$ is about 1.82 times the virial mass estimate, as given in Equation 5 (using the result of Padmanabhan *et al.* 2004).

An important factor that dictates the success of our mass modelling scheme is smoothness of dispersion profiles in real galaxies. As Gebhardt *et al.* (2000) suggested, the

largest variations in normalised dispersions occur in galaxies, either in the inner parts ($R < 0.5X_e$) or at radii exceeding $2X_e$. In the radial range of $0.5X_e < R < 2X_e$, the variations in dispersion profiles is reported to be less than 5%. Gerhard *et al.* (2001) suggest that the M/L profile starts to pick up around $0.5-2X_e$. This uniform dynamical characteristic of real ellipticals is exploited in the production of the formalism.

7.1 Core Fitting Method

At this point, it merits mention that though one part of the proposed mass modelling technique resembles King's core fitting method (King 1966, Rood *et al.* 1972) in some way, the whole of the advanced technique is very different from the core fitting method. The resemblance lies in the invoking of the virial theorem in the extraction of the mass that lies enclosed within a pre-fixed radius; in our work, this is the minimum radius (x_0) at which a velocity dispersion measure is available. In the implementation of the virial theorem, isotropy and sphericity are assumed, as in the core fitting method.

But the essential difference between the two methods lies in the fact that while the virial estimate of the mass is advanced as the answer in the core-fitting method, in our method, this mass is used to spot the range of allowed Υ_{in} values that correspond to this estimate. In other words, given a virial estimate of the mass within x_0 , we attempt to decipher the range of values within which the true central (local) M/L lies. The availability of a range in this M/L offers some respite from the difficulties caused by the possible existence of anisotropy, which the core-fitting method is not safeguarded against; in fact, it appears from work done with real galaxies that this respite is realistic indeed. Moreover, our method would forewarn us in case the system is so severely anisotropic that the method would fail. The core-fitting method has no such inbuilt safeguard.

Most importantly, once we have chosen our Υ_{in} , (which then fixes Υ_{out}), smoothing is implemented. The smoothed mass density distribution is then found to correspond to a local M/L profile that is found to be *different* from the choice of Υ_{in} , in the inner parts of the galaxy. The whole of the M/L distribution, from $x = 0$ to $x = 3X_e$, is rendered affected by the overall smoothing. This is clearly borne by the Figure 4. On the other hand, the M/L in the central parts of the galaxy, as found from the core-fitting method, would of course be just what the virial estimate indicates.

All in all, we can say that our method does invoke the virial theorem to translate velocity dispersion information into an enclosed mass value, as is done in the core-fitting method, but in our technique, we then go ahead to refine that virial estimate in multiple ways, unlike in the core-fitting method. The proposed mass modelling formalism is applicable to aspherical galaxies that are at least as anisotropic in the centre as massive ellipticals in the SDSS, even when these systems bear constant surface brightness cores, and it provides a mass distribution over a radial range extending to about 3 times the effective radius. The core-fitting method is much more constrained in the sense that it provides the mass profile only in the central regions of galaxies that do not harbour a constant surface brightness

core and which when aspherical and/or anisotropic, cause the estimated mass distribution to be erroneous.

7.2 The Case of M87

The fundamental motivation for the raw two-stepped local M/L profile to be ascribed a low inner and high outer M/L amplitude is to replicate the anticipated trend of the dark matter kicking in at large radii ($3X_e$ and higher). But if a system is known (from independent measurements) to harbour a central mass condensation then the innermost radial range should be assigned a high local M/L indeed. Such is the case for the galaxy M87. Additionally, M87 is known to be a cD galaxy lying at the centre of Virgo. Thus, it can be modelled as being bereft of any dark matter, with all the dark matter ascribed to Virgo itself (McLaughlin 1999). Such information about the reported state of the matter distribution in M87 can motivate us to model this galaxy, using our mass modelling scheme, with a two step M/L profile in which the inner M/L amplitude is high, compared to the rest of the radial range covered by photometry. Once we configure our raw M/L profile in this way, the recovered mass distribution in M87 is found to closely follow the mass models predicted for M87 from earlier studies. Thus, the proposed technique relies upon the inclusion of as much measured information about the galaxy at hand, as is possible.

7.3 Connection between luminous & dark matter densities

Once Υ_{in} is constrained, Υ_{out} is fixed; this correlation between Υ_{in} and Υ_{out} depends on whether the system is cored or Sersic. A full investigation was done with the cored galaxies that were normalised to a central luminosity density of $100 L_{\odot} \text{pc}^{-3}$, to suggest that

$$\Upsilon_{out} = 8.32 \times 10^5 r_c^{-3.75} + 9.76 \times 10^8 r_c^{-5.31} \exp \left[\frac{-\Upsilon_{in}}{1.005^{-6} r_c^4 + 1.85} \right]. \quad (7)$$

Similar analysis performed with a toy Sersic brightness profile revealed that Υ_{out} is again related to Υ_{in} via an exponential decay though a more thorough investigation needs to be undertaken to appreciate the dependence of this relation on the Sersic parameters.

The fact that the local mass at $3X_e$ in our toy ellipticals is related uniquely to the mass near the centre, betrays a relationship between the dark matter and luminous matter content in these systems. Given that the total mass density in these models has a contribution from an NFW-type dark halo and α times a (cored or Sersic) luminosity density profile, (where α is a scalar), such a relationship is not altogether unexpected. As shown in Figure 9, it is clear that in the inner regions ($x \leq r_c$) the total mass density is dominated by the shape of the underlying luminosity density profile, while the dark halo predominates in the outer regions ($x \sim 3X_e$). Thus, when the luminous mass is low, the dark mass is high and the vice versa. This trend manifests itself into the exponential decay of the outer M/L value as the inner M/L is increased. It must be kept in mind that this relationship between Υ_{in} and Υ_{out} is in the context of

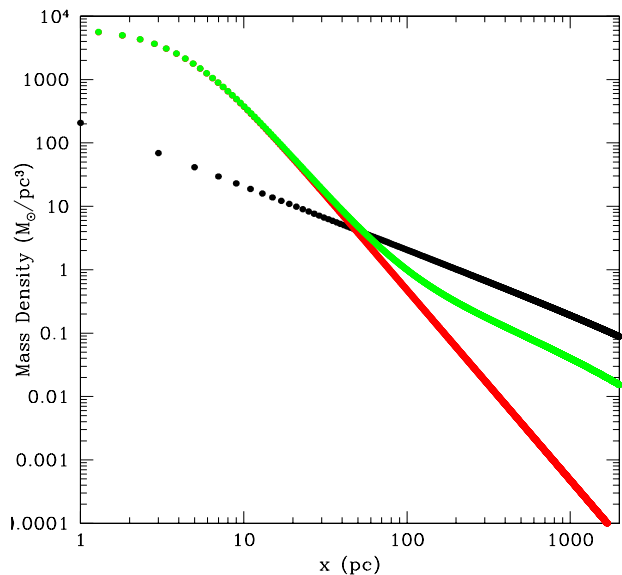


Figure 9. Figure showing trends in dark matter density (black) and luminous matter density (in red) for a model cored galaxy with a core radius of about 14.4pc, eccentricity 0.8 and $\alpha=10$. The sum of these two components is shown in green. The x range spanned in the plot corresponds to thrice the value of X_e for this model galaxy.

the *raw* mass-to-light distribution, while the Figure 9 refers to the situation in the smoothed configuration.

Such a fall-off is also expected for the Sersic galaxies, though the exact nature of the trend with an intrinsic scale length (such as the core radius in case of the cored galaxies) would expectedly differ. But of course, that our *recovered* profiles exhibit this exponential fall-off, indicates the success of our modelling.

7.4 Limitations & Outreach

The more pertinent question is, how general is this trend between the local M/L at the centre and at $3X_e$. In other words, how convincing is the idea that in general there is a quantifiable connection between the luminous matter density in elliptical galaxies and the dark matter content at approximately 3 times the effective radius?

The answer obviously depends on the genericness of the models that we have consulted in our work. As far as the amplitude of the model luminosity densities are concerned, it has been constrained to a value that is typical of the order of magnitude of the central density of real ellipticals. Also, a range of core radii has been scanned successfully in our cored models. Though a range of Sersic type model brightness profiles have not been scanned, the trends noted with the single model Sersic galaxy that was considered here, appear similar in nature to those found for the cored models. Thus, it seems possible that the inner and outer M/L in the raw two-stepped M/L profile will be connected even in the Sersic case, with the exact nature of this connection given by parameters intrinsic to the brightness distribution.

All this corroborates the generality of our models. At the same time it needs to be appreciated that the success

of the procedure depends on the conformity of a real elliptical galaxy to the toy models that were used to set up the rules that connect the inner and outer mass-to-light ratios. In particular, the surface brightness distribution of the real galaxy and the compatibility of its dark halo to the NFW form need to be checked. In fact for each unique family of brightness profiles, a different rule connecting Υ_{in} and Υ_{out} is expected to exist. In this paper, we presented the same for cored galaxies that were normalised to the same central luminosity density and found a similar trend with one toy Sersic galaxy. An extensive study of toy Sersic galaxies is underway, to form a rule similar to the one prescribed in Equation 7. This proposed project will also include an investigation of the effect of changing the nature of the dark matter distribution in the model galaxies, on this rule. Thus, this method can potentially provide a simple automated way of deciphering mass profiles of a large sample of elliptical galaxies.

Thus one important conclusion of this paper is that a connection exists between the inner luminous matter and the dark matter density at about $3R_e$ in cored ellipticals and perhaps also in Sersic galaxies. This notion, though encouraged by intuition, needs to be cultivated better in order to ascertain the physical origin of the accompanying parametrisation.

Similar relationships have been explored in the context of disk galaxies; some of more recent works include contributions from Sancisi (2004), Verheijen (2001) and Noordermer (2006). In these studies and the many more that preceded them, a relationship was noted between the characteristics of the rotation curves and the optical luminosities of disk galaxies. Investigations along similar lines are of course not possible with ellipticals but studies of samples of ellipticals in various catalogues have been undertaken to understand mass distribution in early type systems (Mamon & Lokas 2005, Padmanabhan *et al.* 2004, Lintott, Ferreras & Lahav 2006, among others). The mass modelling technique that is advanced in this paper is one way to pursue the same question, over larger radial ranges than are typically covered in these studies (about 3 effective radii as compared to 1).

Given the simplicity of this method and the twosome observational input required, (which are readily provided by most catalogues, including the SDSS), a future project (Michielsen & Chakrabarty 2006) is planned in which the construction of the mass build up in the nearby universe will be attempted.

ACKNOWLEDGEMENTS

The author is indebted to Michael Merrifield, Chris Conselice and Dolf Michielsen for their helpful comments, and to the anonymous referee whose criticisms and comments helped to shape the work better. The author is funded by a Royal Society Fellowship.

References

Bertola F., Pizzella A., Persic M., Salucci P., 1993. *ApJ*, **416**, 45L.

- Binney J., Tremaine S., 1987. *Galactic Dynamics*, Princeton University Press Princeton New Jersey.
- Buote D. A., Jeltema T. E., Canizares C. R., Garmire G. P., 2002. *ApJ*, **577**, 183.
- Chakrabarty D., Ferrarese L., 2006. *AJ*, , submitted to AJ.
- Chakrabarty D., Portegies Zwart S., 2004. *AJ*, **128**, 1046.
- Chakrabarty D., Saha P., 2001. *AJ*, **122**, 232.
- Côté P., McLaughlin D., Hanes D., Bridges T., Geisler D., Merritt D., Hesser J., Harris G., Lee M., 2001. *ApJ*, **559**, 828.
- Côté P., McLaughlin D. E., Cohen J. G., Blakeslee J. P., 2003. *ApJ*, **591**, 850.
- Ferrarese L., Côté P., Jordan A., Peng E. W., Blakeslee J. P., P. S., Mei S., Merritt D., Milosavljevi M., Tonry J. L., West M. J., 2006. *ApJS*, **164**, 334.
- Gebhardt K., Bender R., Bower G., Dressler A., Faber S. M., Filippenko A. V., Green R., Grillmair C., Ho L. C., Kormendy J., coauthors ., 2000. *ApJ*, **539**, 13L.
- Genzel R., Pichon C., Eckart A., Gerhard O. E., Ott T., 2000. *MNRAS*, **317**, 348.
- Gerhard O., Kronawitter A., Saglia R. P., Bender R., 2001. *AJ*, **121**, 1936.
- Hoekstra H., Yee H. K. C., Gladders M. D., 2004. *ApJ*, **606**, 67.
- King I. R., 1966. *AJ*, **71**, 64.
- Lintott C. J., Ferreras I., Lahav O., 2006. *ApJ*, **648**, 826.
- Macchetto F., Marconi A., Axon D. J., Capetti A., Sparks W., Crane P., 1997. *ApJ*, **489**, 579.
- Mamon G. A., Lokas E. L., 2005. *MNRAS*, **362**, 95.
- McLaughlin D., 1999. *ApJ*, **512**, L9.
- Merritt D., 1993. *ApJ*, **413**, 79.
- Merritt D., 1996. *AJ*, **112**, 1085.
- Michielsen D., Chakrabarty D., 2006. *MNRAS*, , in preparation.
- Napolitano N. R., Capaccioli M., Romanowsky A. J., Douglas N. G., Merrifield M. R., Kuijken K., Arnaboldi M., Gerhard O., Freeman K. C., 2005. *MNRAS*, **357**, 691.
- Noordermer E., 2006. *ApJ*, , in preparation.
- Padmanabhan N., Seljak U., Strauss M. A., Blanton M. R., Kauffmann G., Schlegel D. J., Tremonti C., Bahcall N. A. and Bernardi M., Brinkmann J., Fukugita M., Ivezi ., 2004. *New Astronomy*, **9**, 329.
- Romanowsky A. J., Kochanek C. S., 2001. *ApJ*, **553**, 722.
- Romanowsky A. J., Douglas D. N., Arnaboldi M., Kuijken K., Merrifield M. R., Napolitano N. R., Capaccioli M., Freeman K. C., 2003. *Science*, **301**, 1696.
- Romanowsky A. J., G. D. N., Kuijken K., Merrifield M. R., Arnaboldi A., Napolitano N. R., Merrett H., Capaccioli M., 2004. In: *Dark Matter in Galaxies, Proc. IAU Symposium 220*, 165, eds Ryder S., Pisano D. J., Walker M., Freeman K., ASP, San Francisco.
- Rood H. J., Page T. L., Kintner E. C., King I. R., 1972. *ApJ*, **179**, 627.
- Sancisi R., 2004. In: *International Astronomical Union Symposium no. 220*, 233, eds Ryder S. D., Pisano D. J., Walker M. A., Freeman K., ASP, San Francisco.
- Strom S. E., Strom K. M., Wells D. C., Forte J. C., Smith M. G., Harris W. E., 1981. *ApJ*, **245**, 416.
- van der Marel R. P., 1994. *MNRAS*, **270**, 271.
- Verheijen M. A. W., 2001. *ApJ*, **563**, 694.
- Zepf S. E., Beasley M. A., Bridges T. J., Hanes, D. A. and Sharples R. M., Ashman K. M., Geisler D., 2000. *AJ*, **120**, 2928.